Acta Crystallographica Section B
Structural Science
ISSN 0108-7681

A new polymorph of *ortho*-ethoxy-*trans*-cinnamic acid: single-to-single-crystal phase transformation and mechanism

Manuel A. Fernandes, Demetrius C. Levendis* and F. R. Ludwig Schoening

Molecular Sciences Institute, School of Chemistry, University of the Witwatersrand, PO WITS, 2050 Johannesburg, South Africa

Correspondence e-mail: demi@aurum.chem.wits.ac.za

Received 12 November 2003
Accepted 15 April 2004

The α-polymorph of *ortho*-ethoxy-*trans*-cinnamic acid (OETCA) undergoes a reversible single-crystal-to-single-crystal phase transformation at 333 K. The new high-temperature polymorph (α'-OETCA) is stable between 333 and 393 K with three molecules in the asymmetric unit ($Z' = 3$), space group $P\bar{1}$. Unlike the other polymorphs (and solvate) of OETCA recently reported, two of the molecules in α'-OETCA deviate significantly from planarity. This conformational change results in the corrugated sheet-type structure of α'-OETCA. The sheets are made up of ribbons, each composed of $R_2^2(8)$ hydrogen-bonded pairs (*via* the —COOH groups), which are further connected by CH$\cdots$O interactions. When exposed to UV radiation the α'-OETCA polymorph can be stabilized below 333 K with *ca* 8% of the monomer converted into the photodimer. The crystal structures of α'-OETCA are reported at two temperatures above the phase transition point (at 345 and 375 K) as well as the stabilized forms at 173 and 293 K. A mechanism for the phase transition involving a cooperative conformational transformation coupled with a shift of layers of OETCA molecules is proposed. The α'-OETCA polymorph is also an example of a cinnamic acid derivative where two different potentially photoreactive environments exist in one crystal in which each unit cell has two non-centrosymmetric predimer sites and one centrosymmetric predimer site.

1. Introduction

Although the existence of different *ortho*-ethoxy-*trans*-cinnamic acid (OETCA) polymorphs has been known since 1964, their structures have only recently been reported [Fernandes *et al.*, 2001; Gopalan & Kulkarni, 2001; see (I)]. The solid-state reactivity of many cinnamic acid derivatives was studied and reported in 1964 by Schmidt and his coworkers (Cohen & Schmidt, 1964; Cohen & Green, 1973<). This innovative work led to the formulation of criteria for solid-state [2 + 2] photodimerizations which state that in order for such a reaction to occur, the double bonds involved have to be approximately parallel and between 3.5 and 4.2 Å apart. This distance was based on experimental observations. Although solid-state photodimerization reactions have been intensely studied over the last 40 years there has recently been a renewed interest in reactions of this type (Ito *et al.*, 2003; Varshney *et al.*, 2002; Busse *et al.*, 2002; Tanaka & Toda, 2000; Ohba & Ito, 2003; Hosomi *et al.*, 2000). In these newer studies there has been an emphasis on trying to carry out photodimerization reactions in a single-crystal-to-single-crystal

fashion through the use of tail-end absorbed UV light – a technique first used by Enkelmann and co-workers (Enkelmann *et al.*, 1993). The hope is that through this process some understanding and control over the reaction pathways in the solid state, and hence over the products obtained, will be achieved. There has also been an increasing interest in polymorphism (Bernstein, 2002) and phase changes in the solid state in order to understand the forces keeping crystals together. The study of mechanisms of phase transformations in organic crystals has recently drawn renewed interest with advances significantly aided by the study of single-crystal-to-single-crystal transformations (Hashizume *et al.*, 2003; Botoshansky *et al.*, 1998; Hostettler *et al.*, 1999; Enjalbert & Galy, 2002; Katrusiak, 2000; Kaftory *et al.*, 2001). This work focuses on polymorphism and phase transformations in OETCA. In this paper we report the discovery of a fourth OETCA polymorph (the α'-polymorph) which, although related to its parent α-polymorph, presents new possibilities in the study of photodimerization reactions in the solid state. The dotted arrows in (I) show the relationship between this polymorph and the older polymorphs.[1]

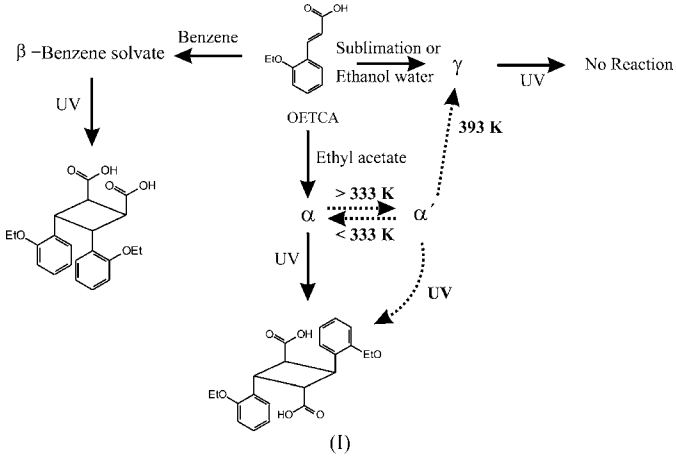

2. Experimental

2.1. Crystal growth

Crystals of the α-polymorph were grown by slow evaporation from a saturated solution of OETCA in ethyl acetate at room temperature (298 K); this produced prism-like crystals. The melting point of these crystals as determined by DSC was 407.9–408.9 K.

2.2. DSC measurements

DSC measurements were carried out using a Standton Redcroft instrument. The measurements were carried out under a nitrogen atmosphere in aluminium crucibles. The sampling rate was 0.10 points s^{-1} and a heating rate of 5° min^{-1} was used.

2.3. High-temperature α'-OETCA polymorph single-crystal analysis

Intensity data were collected at 345 (2) and 375 (2) K using a heating device supplied by Bruker-AXS on a Bruker SMART 1K CCD area-detector diffractometer with graphite-monochromated Mo $K\alpha$ radiation (50 kV, 30 mA). Two crystals with different orientations were used (size: 1.0 × 0.34 × 0.33 and 1.0 × 0.34 × 0.28 mm, respectively; collimator size: 0.8 mm) and a data set at each temperature was collected for each crystal. Large crystals were used to counteract the effect of sublimation at 375 K by allowing quick data collection times (about 1.5 h); smaller crystals were found to have almost disappeared by the time the data collection run was over; alternative methods of preventing sublimation such as coating the crystals with epoxy glue (Hashizume *et al.*, 2003) or sealing in capillaries (Botoshansky *et al.*, 1998) were avoided as they interfered with the phase transition. Two crystals in two different orientations were necessary as the heating device physically restricted the amount of data collected on each crystal to *ca* 60% completeness to 25° θ, for a triclinic unit cell, while collecting two data sets on two crystals mounted in different orientations ensured a data completeness of *ca* 90% to 25° θ. The collection method involved ω scans of width 0.3°. Data reduction was carried out separately on each data set using the program *SAINT*+ (Bruker, 1999*a*) and each dataset was subsequently merged using *XPREP* (Bruker, 1999*a*).

The crystal structure was solved by direct methods using *SHELXTL* (Bruker, 1999*b*). Non-H atoms were first refined isotropically followed by anisotropic refinement by full-matrix least-squares calculations based on F^2 using *SHELXTL*. With the exception of the carboxyl H atoms, all the H atoms were positioned geometrically and allowed to ride on their respective parent atoms. The carboxyl H atoms were located from the difference-Fourier map and allowed to ride on their parent atoms. All H atoms were refined isotropically. In order to ease the discussion of this structure and its potential photodimerization properties, each independent molecule was labeled *A*, *B* or *C*. Crystal data for the α'-polymorph at 345 and 375 K are given in Table 1.

2.4. Stabilized α'-polymorph single-crystal analysis

A sample of the α'-polymorph was stabilized for measurements below the transition temperature (see details below) by placing α-OETCA on a Kofler hot stage at a temperature of 343 (3) K and exposing it to UV light from a Philips TL03 UV lamp for 6 h. Intensity data were collected at 173 (2) and 293 (2) K, as described above.

The crystal structures were solved by direct methods using *SHELXTL* (Bruker, 1999*b*). With the exception of the photodimer, all non-H atoms were first refined isotropically followed by anisotropic refinement by full-matrix least-squares calculations based on F^2 using *SHELXTL*. The

[1] Supplementary data for this paper are available from the IUCr electronic archives (Reference: WS5009), including a videoclip in Quick Time format of the crystal undergoing the phase transition from the α-polymorph to the α'-polymorph, or α' to α, can be downloaded from http://www.gh.wits.ac.za/manuel/transition/. Services for accessing these data are described at the back of the journal.

Table 1
Experimental details.

	At 345 K	At 375 K	Stabilized at 293 K	Stabilized at 293 K
Crystal data				
Chemical formula	$C_{11}H_{12}O_3$	$C_{11}H_{12}O_3$	$2.738C_{11}H_{12}O_3{\cdot}0.131C_{22}H_{24}O_6$	$0.124C_{22}H_{24}O_6{\cdot}2.752C_{11}H_{12}O_3$
M_r	192.21	192.21	576.62	576.62
Cell setting, space group	Triclinic, $P\bar{1}$	Triclinic, $P\bar{1}$	Triclinic, $P\bar{1}$	Triclinic, $P\bar{1}$
a, b, c (Å)	8.7336 (4), 10.9590 (7), 17.2709 (10)	8.7373 (5), 11.0167 (8), 17.2950 (10)	8.6759 (11), 11.0003 (13), 17.299 (2)	8.6452 (13), 10.8577 (17), 17.262 (3)
α, β, γ (°)	91.232 (4), 92.703 (4), 109.472 (4)	91.187 (4), 92.775 (5), 108.938 (4)	92.552 (3), 92.347 (2), 111.155 (3)	92.470 (3), 92.102 (3), 112.563 (3)
V (Å^3)	1555.53 (15)	1571.62 (17)	1535.3 (3)	1492.4 (4)
Z	6	6	2	2
D_x (Mg m^{-3})	1.231	1.218	1.247	1.283
Radiation type	Mo $K\alpha$	Mo $K\alpha$	Mo $K\alpha$	Mo $K\alpha$
No. of reflections for cell parameters	665	797	781	728
θ range (°)	2.7–21.6	2.3–20.9	2.3–21.4	2.4–26.3
μ (mm^{-1})	0.09	0.09	0.09	0.09
Temperature (K)	345 (2)	375 (2)	293 (2)	173 (2)
Crystal form, color	Prismic, colorless	Prismic, colorless	Irregular, white	Irregular, white
Crystal size (mm)	1.00 × 0.34 × 0.31	1.00 × 0.34 × 0.31	0.38 × 0.33 × 0.26	0.38 × 0.33 × 0.24
Data collection				
Diffractometer	Bruker SMART1K	Bruker SMART1K	Bruker SMART1K	Bruker SMART1K
Data collection method	ω scans with 0.3 ° steps at χ = 57.4°	ω scans with 0.3 ° steps at χ = 57.4°	ω scans with 0.3 ° steps at χ = 57.4°	ω scans with 0.3 ° steps at χ = 57.4°
Absorption correction	None	None	None	None
No. of measured, independent and observed reflections	4937, 4937, 2689	4947, 4947, 1906	8251, 5391, 2192	8177, 5500, 3167
Criterion for observed reflections	$I > 2\sigma(I)$	$I > 2\sigma(I)$	$I > 2\sigma(I)$	$I > 2\sigma(I)$
R_{int}	0.000	0.000	0.028	0.022
θ_{max} (°)	25.0	25.0	25.0	25.5
Range of h, k, l	$-10 \Rightarrow h \Rightarrow 10$ $-12 \Rightarrow k \Rightarrow 12$ $0 \Rightarrow l \Rightarrow 20$	$-10 \Rightarrow h \Rightarrow 10$ $-12 \Rightarrow k \Rightarrow 12$ $0 \Rightarrow l \Rightarrow 20$	$-10 \Rightarrow h \Rightarrow 10$ $-11 \Rightarrow k \Rightarrow 13$ $-20 \Rightarrow l \Rightarrow 14$	$-10 \Rightarrow h \Rightarrow 8$ $-13 \Rightarrow k \Rightarrow 13$ $-20 \Rightarrow l \Rightarrow 20$
Refinement				
Refinement on	F^2	F^2	F^2	F^2
$R[F^2 > 2\sigma(F^2)]$, $wR(F^2)$, S	0.049, 0.152, 1.02	0.049, 0.157, 0.88	0.068, 0.220, 0.90	0.053, 0.136, 1.03
No. of reflections	4937	4947	5391	5500
No. of parameters	386	386	391	390
H-atom treatment	Mixture of independent and constrained refinement	Mixture of independent and constrained refinement	Mixture of independent and constrained refinement	Mixture of independent and constrained refinement
Weighting scheme	$w = 1/[\sigma^2(F_o^2) + (0.0807P)^2 + 0.0096P]$, where $P = (F_o^2 + 2F_c^2)/3$	$w = 1/[\sigma^2(F_o^2) + (0.0788P)^2]$, where $P = (F_o^2 + 2F_c^2)/3$	$w = 1/[\sigma^2(F_o^2) + (0.1128P)^2]$, where $P = (F_o^2 + 2F_c^2)/3$	$w = 1/[\sigma^2(F_o^2) + (0.0572P)^2 + 0.0749P]$, where $P = (F_o^2 + 2F_c^2)/3$
$(\Delta/\sigma)_{max}$	<0.0001	<0.0001	<0.0001	<0.0001
$\Delta\rho_{max}$, $\Delta\rho_{min}$ (e Å^{-3})	0.16, −0.12	0.15, −0.11	0.19, −0.18	0.14, −0.21
Extinction method	*SHELXL*	*SHELXL*	*SHELXL*	None
Extinction coefficient	0.0085 (17)	0.0062 (13)	0.008 (2)	–

Computer programs: *SMART* (Bruker, 1998), *SAINT*+ (Bruker 1999*a*), *SHELXTL* (Bruker, 1999*b*), *PLATON* (Spek, 2003), *SCHAKAL*-97 (Keller, 1997), *DS ViewerPro* (Accelrys Inc., 2002).

photodimer was refined isotropically as a rigid body. All H atoms were first located from the difference map then positioned geometrically and allowed to ride on their respective parent atoms. All H atoms were refined isotropically.

Each molecule was assigned a label such that molecules *A*, *B* and *C* (see §2.3) refer to the equivalent molecule in the α'-polymorph. The final occupancies for molecules *A*, *B*, *C* and the photodimer (in the reaction site formed by molecules *A* and *B*) were 0.869 (3), 0.869 (3), 1, 0.131 (3) and 0.876 (2), 0.876 (2), 1, 0.124 (2) at 293 and 173 K, respectively. Crystal data for the stabilized α'-polymorph at 173 and 293 K are given in Table 1.

3. Results and discussion

3.1. Thermal analysis studies

Thermal analysis of the α-polymorph *via* DSC revealed an endothermic peak at 336 K (onset temperature 333 K; Fig. 1). DSC traces for the β- and γ-forms of OETCA revealed no

such peak, implying that this transition is unique to the α-polymorph. The melting-point measurements for the α-form led to the observation that heating up a single crystal above 333 K would cause it to 'hop' or jump. This was a consistent result since it would occur with every fresh α-crystal used. This hopping phenomenon, alternatively referred to as the thermosalient effect (Bernstein, 2002), has also been observed in *ttatt*-perhydropyrene (Ding *et al.*, 1991) and 1,2,4,5-tetrabromobenzene (Lieberman *et al.*, 2000) amongst others. Cooling the crystals down and heating them up again did not reproduce the 'hopping' effect, implying that there is a difference in the state of the α-crystal before and after the first phase transition. However, DSC scans of samples that had been repeatedly cooled and heated around the 336 K peak revealed that the phase transition is reversible.

Following the phase transition *via* hot-stage optical microscopy confirmed that this phase change was completely reversible, with the crystals remaining intact after several phase transformations (Figs. 2*a* and *b*), even though the crystal dimensions changed by *ca* 10% as a consequence of the transformation.

X-ray diffraction rotation photographs taken before and after the phase transitions (Fig. 3) showed that the diffraction patterns differed significantly in detail, but were obviously related to each other. The two large diffraction spots in Fig. 3(*a*) are the $(\bar{1}02)$ reflections and correspond to the molecular layers in the α-polymorph. Since the three layers in this structure have an identical *d*-spacing a strong reflection spot is observed (see Fernandes *et al.*, 2001.). After the phase transition to the α'-polymorph this peak splits (Fig. 3*b*).

Heating a crystal of the α'-polymorph would cause a front to move through the crystal at around 393 K, which after further examination was found to be due to a phase transition to the γ-polymorph. The crystal now appeared more opaque than before and the phase transition was found to be irreversible. Heat changes corresponding to this transition were not picked up by DSC (DSC traces were carried out on various makes of machines), which is remarkable as the structures differ significantly from each other (the α'-polymorph has a layered structure while the γ-polymorph has a herringbone-type structure). Further heating led to the normal melting of the crystal at 407–409 K. The X-ray diffractogram of the crystal after undergoing a phase transition to the γ-polymorph is shown in Fig. 3(*c*). It is quite evident that the crystal is now a polycrystalline sample as the diffractogram almost looks like a powder pattern. The identity of this phase was confirmed by X-ray powder diffraction.

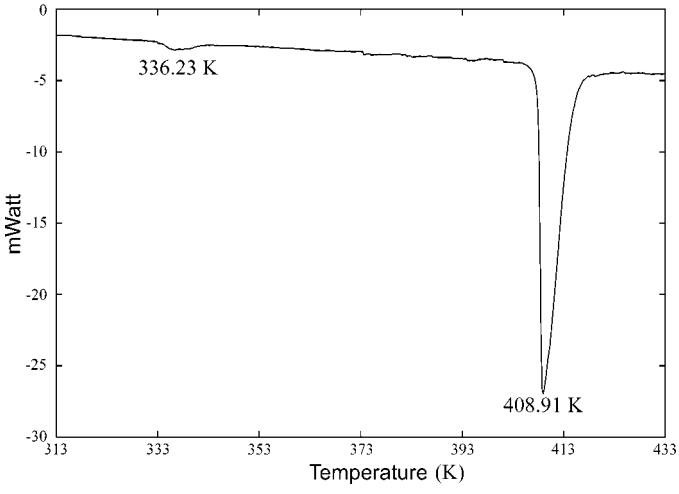

Figure 1
DSC scan showing a peak at 336 K where the *a* polymorph transforms to the α'-polymorph which undergoes a phase transition to the α-polymorph. The melting point peak is at 408.9 K.

3.2. The naming of this new polymorph

In naming this new polymorph two possibilities were considered:

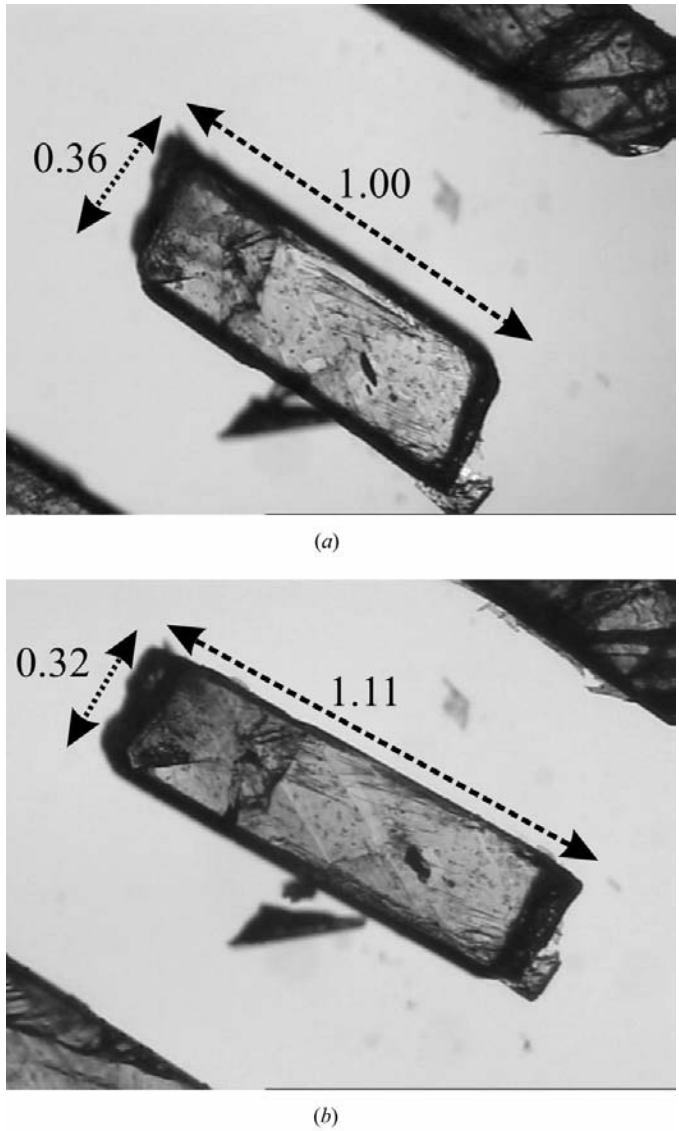

Figure 2
An α-polymorph crystal (293 K) (*a*) before and (*b*) after (~345 K) the phase transition to the α'-polymorph as photographed on an optical microscope. Approximate crystal dimensions (arbitrary units) indicate that the crystal dimensions change by *ca* 10% during this process.

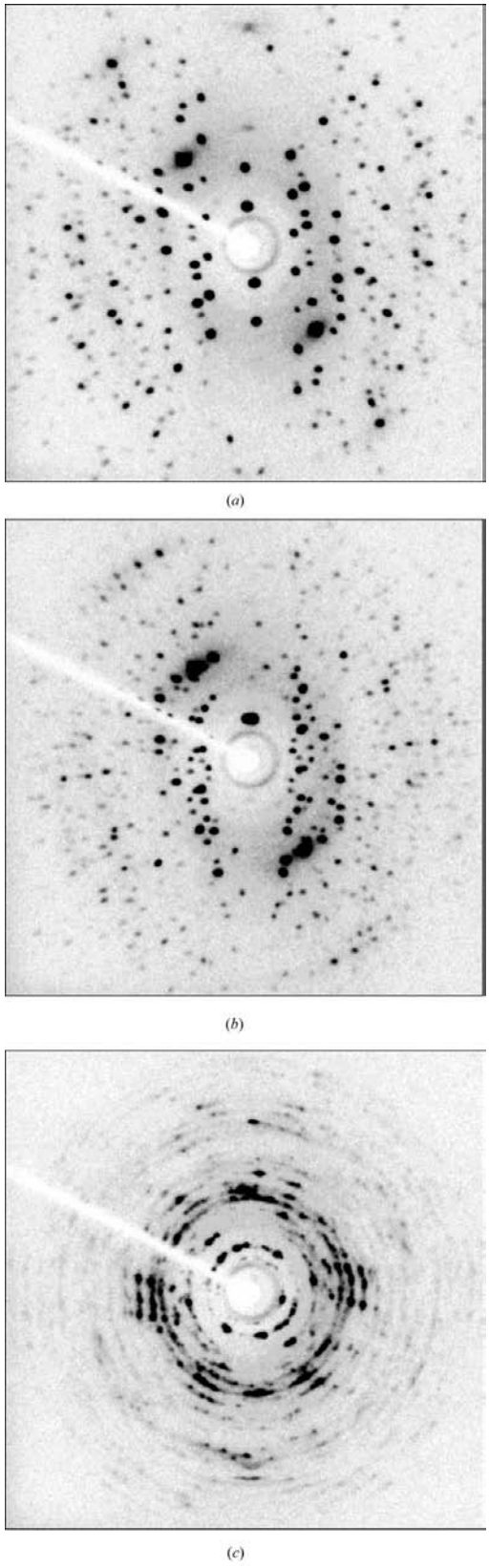

Figure 3
Diffractograms from (*a*) the α-polymorph crystal before the phase transition; (*b*) after the reversible phase transition to the α'-polymorph; (*c*) after the irreversible phase change to the γ-polymorph.

(i) that it be labelled the δ-polymorph since it is the fourth known polymorph of OETCA (a system that seems to be most in use today), or

(ii) that the new polymorph be labelled as the α'-polymorph, indicating that it is related to the α-polymorph through a reversible phase transition. In addition, both these polymorphs yield the same centrosymmetric photochemical product (making it an α-polymorph according to the Schmidt labelling method; Cohen & Schmidt, 1964; Cohen & Green, 1973) and have the shortest cell axes greater than 5.1 Å (making it an α-polymorph according to the Hung labelling method; Hung *et al.*, 1972).

After examining both possibilities it was decided that the new polymorph should be labelled as the α'-polymorph so as to show the origin of the polymorph as well as to show its relationship to the other polymorphs of cinnamic acid in terms of its photochemical product and cell dimensions.

3.3. Molecular structure

ORTEP diagrams for the three molecules in the α'-polymorph are shown as Fig. 4. As would be expected the thermal displacement parameters for the molecules are significantly larger than those for the room- and low-temperature[2] structures – the average U_{iso} value (average isotropic atomic displacement parameter for all the C and O atoms in the asymmetric unit only) is 0.03 at −173 K, 0.06 at 293 K, 0.09 at 345 K and 0.11 at 375 K. There is, however, very little difference between the 345 and 375 K α'-structures as the r.m.s. (root-mean square) deviation between the asymmetric units at the two temperatures is only 0.021 Å. From the point of view of the phase transition, this indicates that very little extra change occurs after the phase transition from the α-polymorph and that changes in the molecular structure occur only during the phase transition itself. As is expected, the cell volume at 375 K is larger than at 345 K (Table 1), but only by *ca* 1%.

Unlike the other OETCA polymorphs, two of the three molecules in the α'-asymmetric unit (Fig. 5) deviate from planarity. The deviations are due to rotations around the C2—O21 and O21—C21 bonds in the ethoxy group, and the C12—C13 bond in the carboxylic side chain. For comparison purposes these torsion angles as well as the mean deviation from planarity (for C and O atoms only) are given together with those from the α-polymorph at 173 K in Table 2. It is quite apparent that molecule *A* shows the least deviation from planarity and the least deviation compared with the parent α-polymorph molecule. This molecule is still essentially flat as the maximum deviation in the torsion angles (from 0 or 180° depending on the torsion angle) is 3.2°. Molecule *B* shows a much greater planar deviation due to a twist in the carboxylic acid group – the C11—C12—C13—O12 torsion angle is 6.8° – while the maximum torsional deviation (from 0 or 180°) in the ethoxy group is only 2.6°. Although molecule *C* has a slightly

[2] For comparison purposes room- and low-temperature U_{iso} values were obtained from the α-polymorph and not from the stabilized α-structures mentioned above.

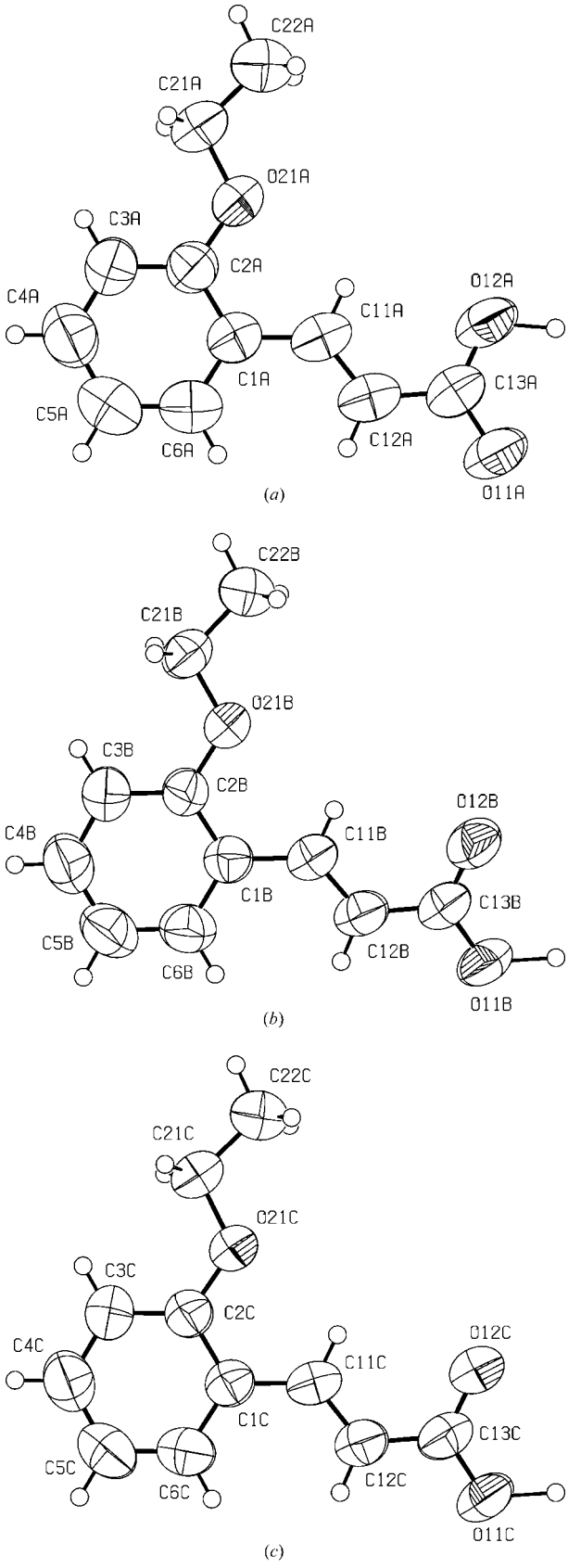

Figure 4
ORTEP (50% ellipsoids) diagrams of the three independent OETCA molecules from the α'-polymorph at 345 K. Diagrams for the 375 K structure are almost identical.

smaller planar deviation than molecule *B*, torsion angle deviations (from 0 or 180°) are present in both the ethoxy and carboxylic acid groups. The deviation is especially pronounced in that the ethoxy group (C2—O21—C21—C22) deviates from 180° by *ca* 8.5°. Although the torsion angle differences and planar deviations are generally small they have a significant impact on the structure of the α'-polymorph.

3.4. Classical hydrogen bonding

Like the other known OETCA polymorphs, classical hydrogen bonding (O—H···O) only occurs between the carboxylic acid groups on two adjacent OETCA molecules forming $R_2^2(8)$ hydrogen-bonded carboxylic acid dimer pairs (Fig. 6). In the α'-polymorph *A* molecules hydrogen bond to other *A* molecules across a centre of inversion to form centrosymmetric *AA* hydrogen-bonded dimers, *i.e.* they have a first-level graph set of $R_2^2(8)$. In contrast, *B* molecules

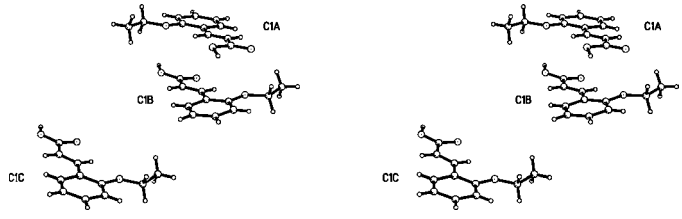

Figure 5
Stereo diagram of the asymmetric unit of the α'-polymorph at 345 K showing the non-planar conformation of two of the three independent OETCA molecules. With the exception of the position of the carboxylic H atoms on molecule *B* and *C* the structure is identical to the 375 K structure.

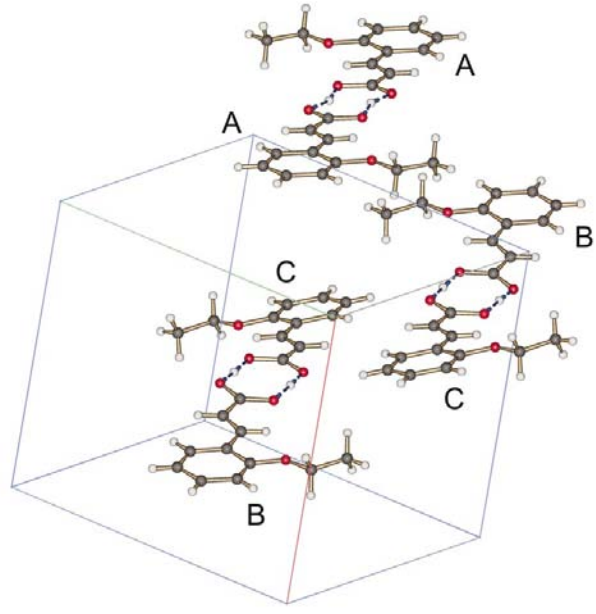

Figure 6
The two types of hydrogen-bonded carboxylic acid dimer pairs from the α'-polymorph at 345 K. For each centrosymmetric *AA* pair (see text) there are two non-centrosymmetric *BC* pairs.

Table 2
Selected torsion angles (°) and mean deviation from planarity (Å) for molecules *A*, *B* and *C* from the α'-polymorph at 345 K and the α-polymorph at 173 K.

Molecule	C11—C12—C13—O12	C2—O21—C21—C22	C3—C2—O21—C21	Planar deviation
A	−0.7 (4)	176.8 (2)	1.1 (3)	0.0180
B	6.8 (3)	−177.41 (17)	−1.3 (3)	0.0678
C	3.6 (4)	−171.53 (19)	−7.1 (3)	0.0606
α-Polymorph	−4.1 (3)	179.01 (17)	−1.8 (3)	0.0296

Table 3
Oxygen to oxygen distances for the carboxylic acid hydrogen-bond dimers in the α'-polymorph at 345 and 375 K and in the stabilized α'-polymorph at 173 and 293 K.

Data from the α- and γ-polymorphs (both structures collected at 173 K; Fernandes *et al.*, 2001) have been included for comparison.

High-temperature collection	O···O	*d*(O···O) (Å)	Stabilized crystals	O···O	*d*(O···O) (Å)
345 K	O12*A*···O11*A*^{i}	2.626 (3)	173 K	O12*A*···O11*A*^{i}	2.566 (3)
345 K	O12*B*···O11*C*^{ii}	2.635 (2)	173 K	O12*B*···O11*C*^{ii}	2.622 (3)
345 K	O12*C*···O11*B*^{ii}	2.642 (2)	173 K	O12*C*···O11*B*^{ii}	2.591 (2)
375 K	O12*A*···O11*A*^{i}	2.630 (3)	293 K	O12*A*···O11*A*^{i}	2.578 (6)
375 K	O12*B*···O11*C*^{ii}	2.646 (3)	293 K	O12*B*···O11*C*^{ii}	2.618 (4)
375 K	O12*C*···O11*B*^{ii}	2.640 (3)	293 K	O12*C*···O11*B*^{ii}	2.593 (4)
α (173 K)	O12···O11^{iii}	2.637 (2)	γ (173 K)	O12···O11^{iii}	2.6241 (17)

Symmetry codes: (i) $-x+1, -y, -z$; (ii) $-x+2, -y+1, -z+1$; (iii) $-x+2, -y, -z+1$.

hydrogen bond to *C* molecules to form non-centrosymmetric *BC* hydrogen-bonded dimers. Using the graph-set notation first introduced by Etter (1990) and elaborated on by Bernstein *et al.* (1995), the first-level graph set for this hydrogen bond is *DD* (where each carboxylic acid hydrogen bond is unique due to the lack of an inversion centre) and $R_2^2(8)$ is obtained only when second-level graph sets are examined.

As explained in §2, the hydrogen-bond data given in Table 3 were obtained by locating the carboxylic H-atom positions in the difference map and then fixing them to their parent atom. In contrast to the usual O—H bond length of *ca* 0.82 Å (the default for *SHELXTL* at 345 K), O—H lengths in the α'-polymorph at 345/375 K are on average *ca* 1.21/1.28 Å long or *ca* 46/48% of the O···O distance (average 2.63/2.64 Å), respectively, *i.e.* the H atoms are almost in the middle of the hydrogen bond being shared almost equally between two carboxylic O atoms. Since being in the middle of the carboxylic acid bond would maximize the repulsion energy between the two carboxylic H atoms, it is more likely that this is really an average situation with the H atoms being disordered on both sides of this position. Such a situation exists in the γ-polymorph where the carboxylic H atom is disordered over the two carboxylic atom sites in an almost 50:50 ratio (see Fernandes *et al.*, 2001). Although the use of X-ray diffraction is not a good method to study the dependence of the position of the H atom with temperature, such experiments have been carried out using neutron diffraction for benzoic acid (Wilson *et al.*, 1996*a*,*b*) and acetylsalicylic acid (Wilson, 2001). The results of these detailed analyses revealed that the disorder (or alternatively anomalous thermal motion) in the hydrogen position between the donor and acceptor atoms does have a dependence on temperature in both these compounds. Close examination of the difference-Fourier maps for the α'-polymorph at 345 K indicates that the location of the carboxylic H atoms is spread out between the two carboxylic O atoms, with the maximum being close to the middle of each O···O pair. When compared with difference maps for the γ-polymorph at 173 K it is noticeable that the picture is very similar. One could speculate that the position of the carboxylic H atoms in the γ-polymorph are influenced by crystal growth and cooling conditions, noting our observation that the γ-polymorph can only be grown from solutions at temperatures above 333 K.

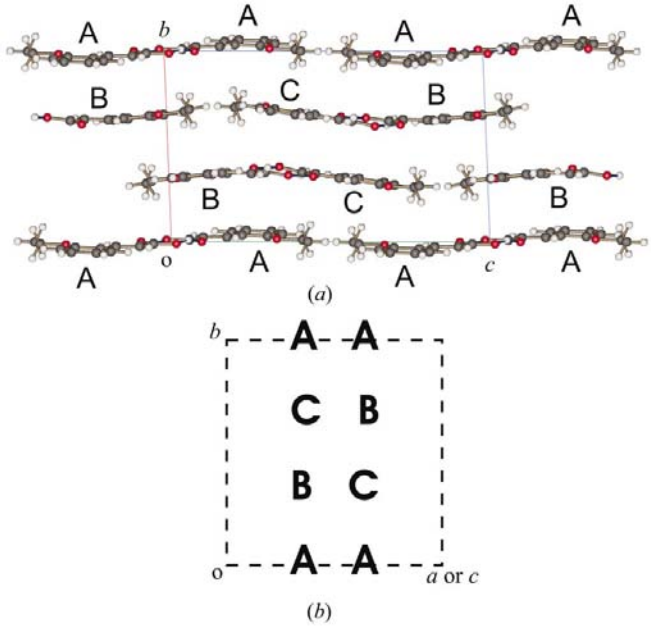

Figure 7
Unit cell of the α'-polymorph as a projection down the *a*-axis, showing the corrugated sheets. The unit cell is represented in schematic form in (*b*).

3.5. Crystal packing

Molecules in the α'-polymorph pack as corrugated sheets (Fig. 7). There are two types of 'sheets' – one composed of *A* molecules (the *AA* sheet) and the other composed of *B* and *C*

Table 4
CH···O (as C···O) distances for ribbons from the α'- (345 K structure), α- and γ- (both at 173 K) polymorphs.

In all cases O12···C5 and O11···C6 refer to the same contacts in each of the three structures.

	C···O (Å)
α'-Polymorph/*BC* ribbon	
O12*c*···C5*c*	3.654 (3)[i]
O11*b*···C6*c*	3.417 (3)[ii]
O12*b*···C5*b*	3.699 (3)[i]
O11*c*···C6*b*	3.507 (3)[ii]
α'-Polymorph/*AA* ribbon	
O12*a*···C5*a*	3.656 (4)[iii]
O11*a*···C6*a*	3.443 (3)[iv]
α-Polymorph	
O12···C5	3.645 (3)[v]
O11···C6	3.413 (3)[vi]
γ-Polymorph	
O12···C5	3.665 (2)[vii]
O11···C6	3.403 (2)[viii]

Symmetry codes: (i) $x-1, y, z$; (ii) $-x+1, -y+1, -z+1$; (iii) $x+1, y, z$; (iv) $-x+2, -y, -z$; (v) $x, y-1, z$; (vi) $-x+2, -y-1, -z+1$; (vii) $x-\frac{1}{2}, y-\frac{1}{2}, z$; (viii) $-x, -y+3, -z$.

molecules (the *BC* sheet). This is because of the reduction in symmetry in undergoing a phase change from the α-polymorph (with one molecule in the asymmetric unit) to the α'-polymorph (with three molecules in the asymmetric unit). There are two *BC* sheets to each *AA* sheet resulting in an *AA*–*CB*–*BC*–*AA*... sequence of sheets along the *b*-axis (Fig. 7). The corrugated packing is due to the lack of planarity in the OETCA molecules, with the *AA* sheet being more flat than the *BC* sheets due to the *B* and *C* molecules having a higher deviation from planarity. Both OETCA 'sheets' have a strong resemblance to the layers of the α-polymorph – a similarity that allows the two phases to interchange depending on the temperature of the crystal. Like the layers in the α -and γ-polymorphs, each sheet is composed of ribbons of OETCA molecules kept together by weak CH···O interactions which have identical geometries to those in the α- and γ-polymorphs (Table 4 and Fig. 8), but have different O—H···O and C—H···O distances. These ribbons also have some level of curvature – the *AA* ribbons are S-shaped, while the *BC* ribbons are U-shaped when viewed down the *a*-axis; those in the α- and γ-polymorphs are flat.

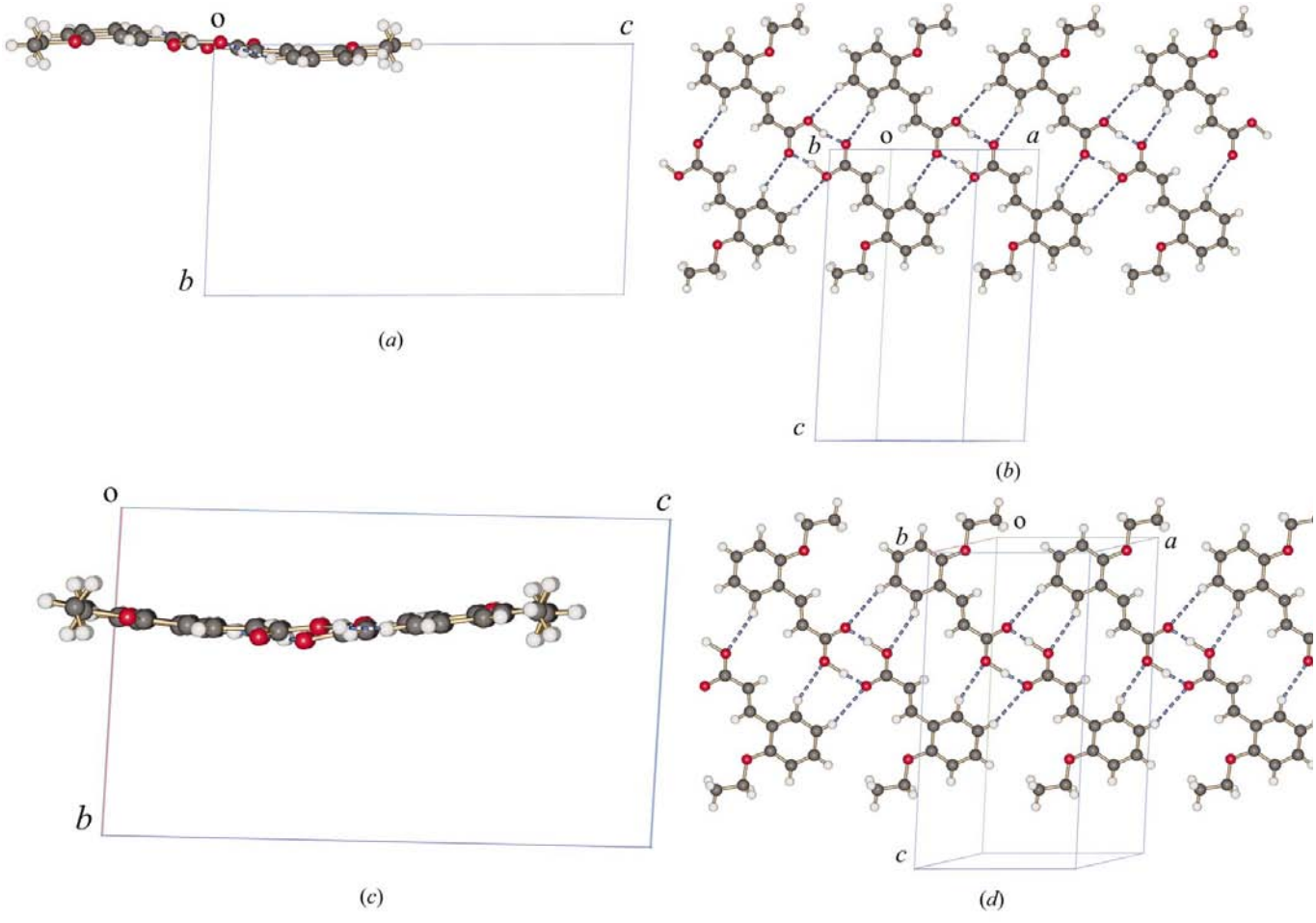

Figure 8
O—H···O and C—H···O ribbon motifs from the α'-polymorph viewed down the *a*-axis and perpendicular to the ribbon: (*a*) and (*b*) the centrosymmetric S-shaped *AA* ribbon; (*c*) and (*d*) the non-centrosymmetric U-shaped BC ribbon.

Table 5
Cell parameters for the α-polymorph (original unit cell), the alternative, transformed unit cell (α_{trans}, after applying the matrix [0$\bar{1}$0/$\bar{1}$01/2$\bar{1}\bar{1}$]) and the α'-polymorph.

Polymorph	α	α (transformed cell)	α'
Space group	$P\bar{1}$	$P\bar{1}$	$P\bar{1}$
Z	2	6	6
a (Å)	6.6992 (6)	8.6807 (8)	8.7336 (4)
b (Å)	8.6807 (8)	10.1254 (8)	10.9590 (7)
c (Å)	10.0151 (9)	17.2967 (12)	17.2709 (10)
α (°)	72.019 (2)	98.850 (7)	91.232 (4)
β (°)	71.464 (2)	91.793 (4)	92.703 (4)
γ (°)	67.867 (2)	93.214 (3)	109.472 (4)

3.6. Closest distances between the reactive double bonds in the α'-polymorph

The α'-polymorph is an example of a cinnamic acid derivative where two different photochemical reaction environments exist in one crystal (Fig. 9). Specifically, each unit cell in this polymorph has two non-centrosymmetric 'pre-photodimer' (hereafter referred to as predimer) sites, the *AB* pairs and one centrosymmetric site (the *CC* pair). Molecules in the non-centrosymmetric sites have an average predimer double-bond contact distance of 3.72 Å (at 345 K) – a distance within the Schmidt criterion distance of 3.5–4.2 Å potentially leading to the centrosymmetric OETCA dimer product. Molecules in the centrosymmetric sites have a predimer double bond contact distance of 4.99 Å (at 345 K) – a distance outside the Schmidt criterion distance and implying that this pair should be light stable. This difference in distances is a direct consequence of the reduction of symmetry.

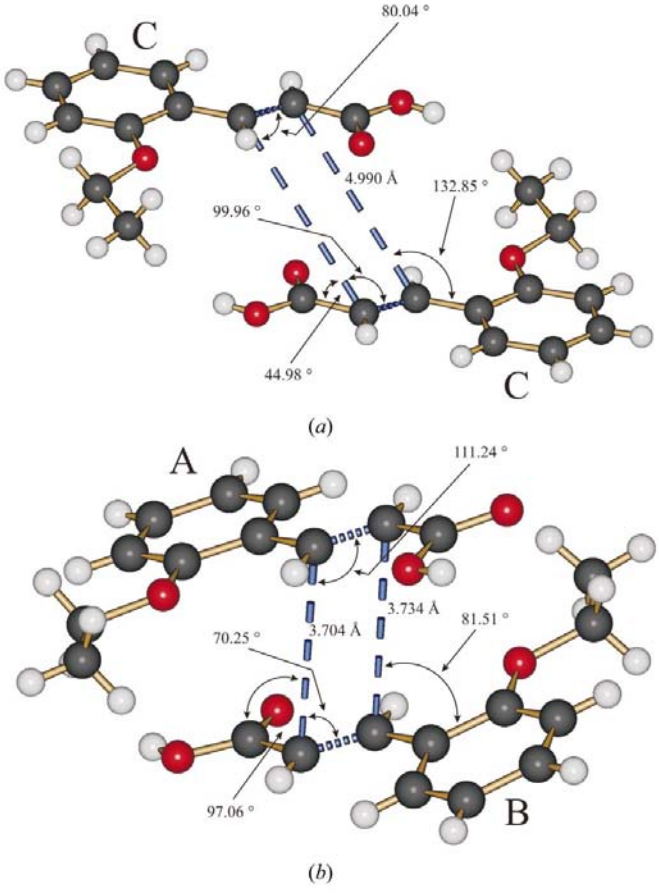

Figure 9
Predimer pairs from the α'-polymorph showing geometries at 345 K of (*a*) the centrosymmetric *CC* pair and (*b*) the non-centrosymmetric *AB* pair.

3.7. Stabilizing the α'-polymorph

A study of the solid-state photochemistry of α'-OETCA (Fernandes & Levendis, 2004) revealed that low levels of reaction, where only about 8% of the monomer had been reacted, stabilized the metastable α'-polymorph enabling a single-crystal diffraction study at 173 K. In contrast, the unreacted α'-polymorph undergoes a phase change back to the α-polymorph at temperatures below 333 K. Plots of cell parameters for the α'-polymorph before and after stabilization at various temperatures are shown in Fig. 10. These indicate that such a stabilization process does not change the cell parameters much while allowing one to experimentally measure such data at temperatures well below the phase transition temperature. The range in the cell axes and cell angles at the temperatures studied are 0.16 Å and 3.09°, respectively.

It was also revealed that, at least initially, a single-crystal-to-single-crystal reaction occurs in the *AB* reaction site (Fig. 11).

Stabilization of the α'-polymorph is possible because photodimerization effectively clips the *AA* and *BC* sheets together, preventing the molecular movement required to change back to the α-polymorph. It is also notable that the *BC* sheets do not move much relative to each other when the stabilized structure has been cooled to 173 K, suggesting that the relationship between the *BC* sheets is a relatively stable one. However, the stabilization of the relative position of BC sheets is not fixed, as shown by the abrupt decrease in the C11*C*···C12*C* predimer distance from the α'-polymorph to the stabilized α'-polymorphs (indicated by Δ in Fig. 10).

3.8. Phase change mechanism: comparing the α- and α'-polymorphs

The relationship between the cell vectors of the α and α'-polymorph are as follows

$$\mathbf{a}_{\alpha'} = -\mathbf{b}_{\alpha}$$
$$\mathbf{b}_{\alpha'} = -\mathbf{a}_{\alpha} + \mathbf{c}_{\alpha}$$
$$\mathbf{c}_{\alpha'} = -2\mathbf{a}_{\alpha} + \mathbf{b}_{\alpha} - \mathbf{c}_{\alpha}$$

This geometrical relationship is shown graphically in Fig. 12, while the effect of applying it to the unit-cell parameters of the α-polymorph (see Fernandes *et al.*, 2001) is given in Table 5.

While the untransformed α-polymorph has one axis lying in the layer plane (the *b*-axis) and two pointing between the molecular layers (the *a*- and *c*-axes), the transformed α-polymorph has two axes in the layer plane (the *a*- and *c*-axes) and one axis pointing into the layer planes (Fig. 12).

Packing diagrams comparing the α- and α'-polymorphs are shown in Figs. 13–15, viewed down the *a*-, *c*- and *b*-axes, respectively. Overlapping the transformed α- (hereafter

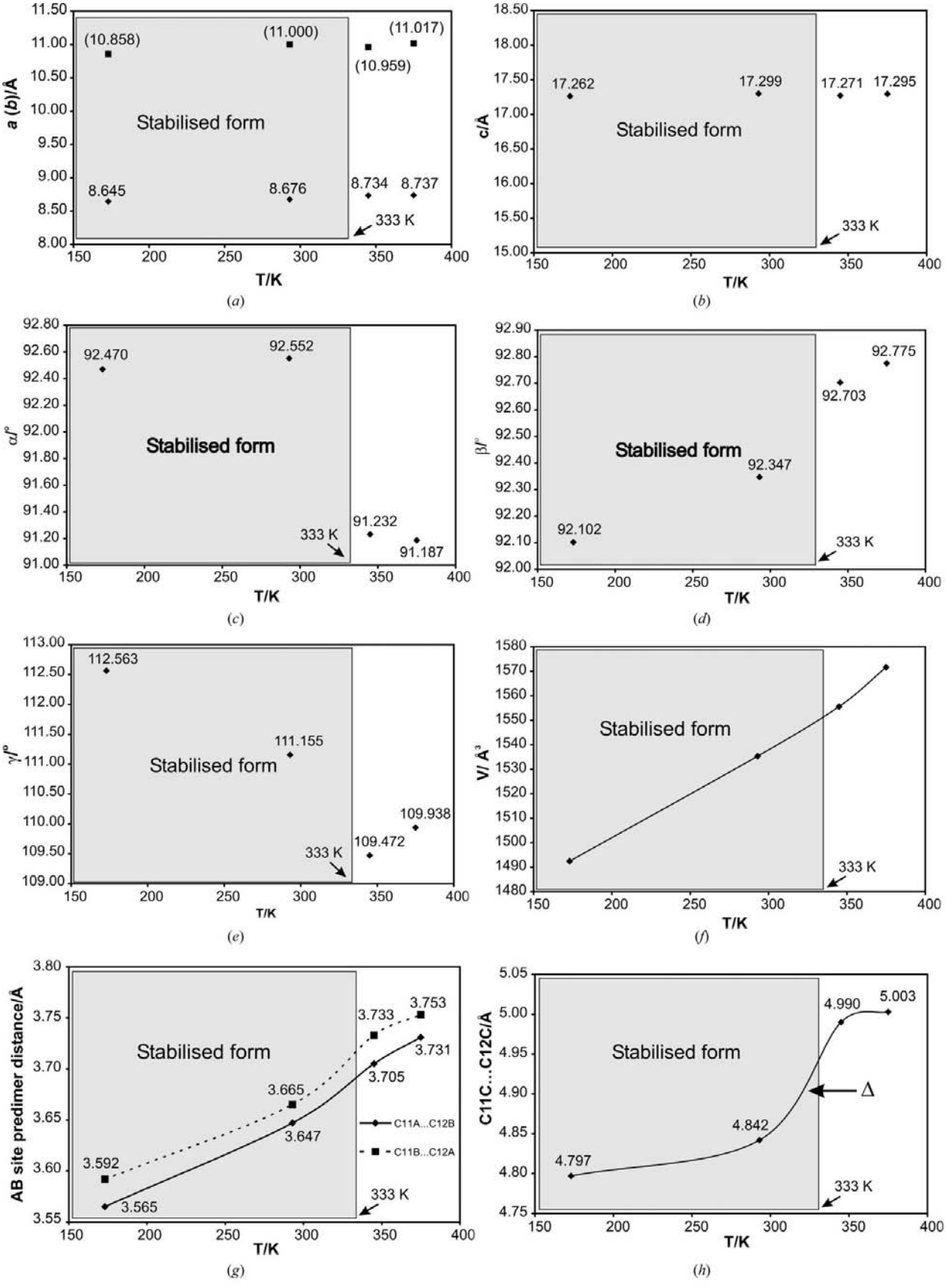

Figure 10
Plot of the unit-cell parameters and specific predimer contacts *versus* temperature (in Kelvin) for the α'-polymorph (measured at 345 and 375 K) and after stabilization (measured at 173 and 293 K).

referred to as α_{trans}) and α'-polymorphs and viewing down the *a*-axis indicates the OETCA molecules do not move much along the *b*- and *c*-axes (Fig. 13) during the phase change. Instead it is obvious that they deviate from planarity in this view. The α angle does however change by *ca* 7.6°. Closely examining the relative positions of the OETCA ethoxy groups in the upper and lower layers of each unit cell in Fig. 13 indicates the type and amount of movement involved. Nonetheless, the molecular movements involved are minimal when compared with movements along the *a*-axis (Fig. 14). In this case the γ angle changes by *ca* 16°. Close examination of the unit-cell diagrams in Figs. 14(*a*) and (*b*) indicates that the two *BC* sheets retain their relative orientation, while the *AA* sheets have undergone significant movements along *a* relative to the *BC* sheets. The *BC* layers are altered a little by the phase change (Figs. 14*c* and 15*a*). In contrast, the OETCA molecules in the *AA* layers move *ca* 2.7 Å (indicated by an X in Figs. 15*b* and *c*) along the *a*-axis. This reveals one aspect of the phase transition mechanism. Effectively each *BC* pair moves around an *AA* layer in a concerted and centrosymmetric fashion, a consequence of the pre-*AA* layer being centrosymmetrically related to the layers above and below. The optical observation of a crystal undergoing a phase

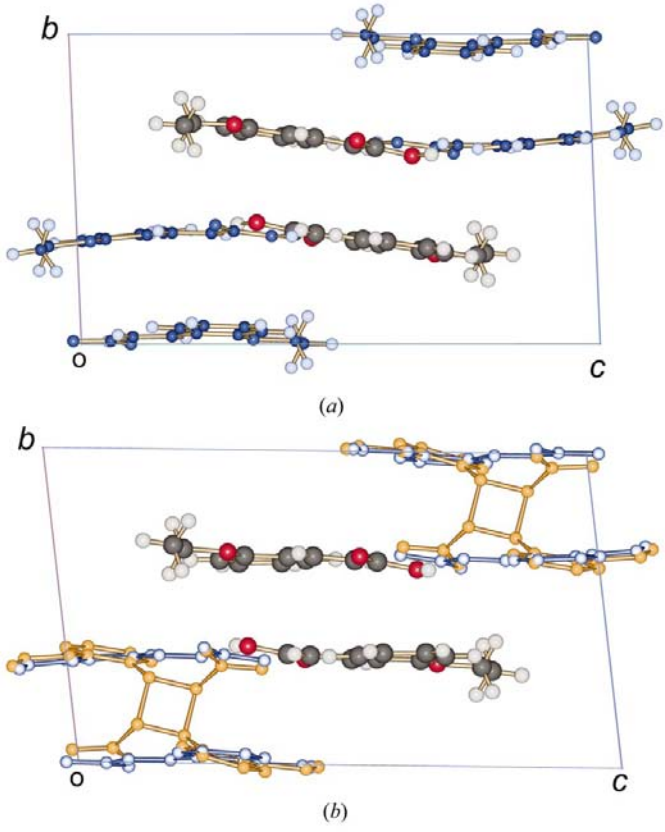

Figure 11
The α'-polymorph, at 375 K, (*a*) before and (*b*) after 6 h of exposure to UV light at 343 K showing the photodimer molecule in the *AB* reaction site.

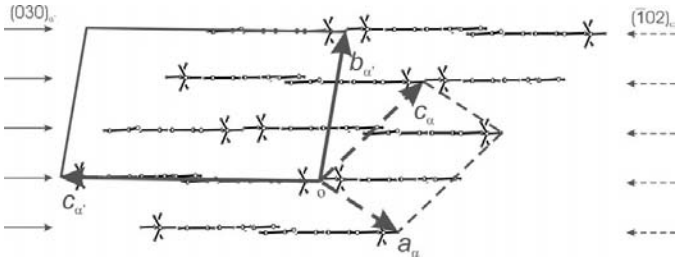

Figure 12
Geometric cell relationships between the α (dotted lines) and α'-polymorphs (solid lines) superimposed on a packing diagram from the α-polymorph. Cell axes b_α and $a_{\alpha'}$ lie perpendicular to the page but point in opposite directions. The $\bar{1}02$ plane in the α-polymorph corresponds to the 030 plane in the α'-polymorph.

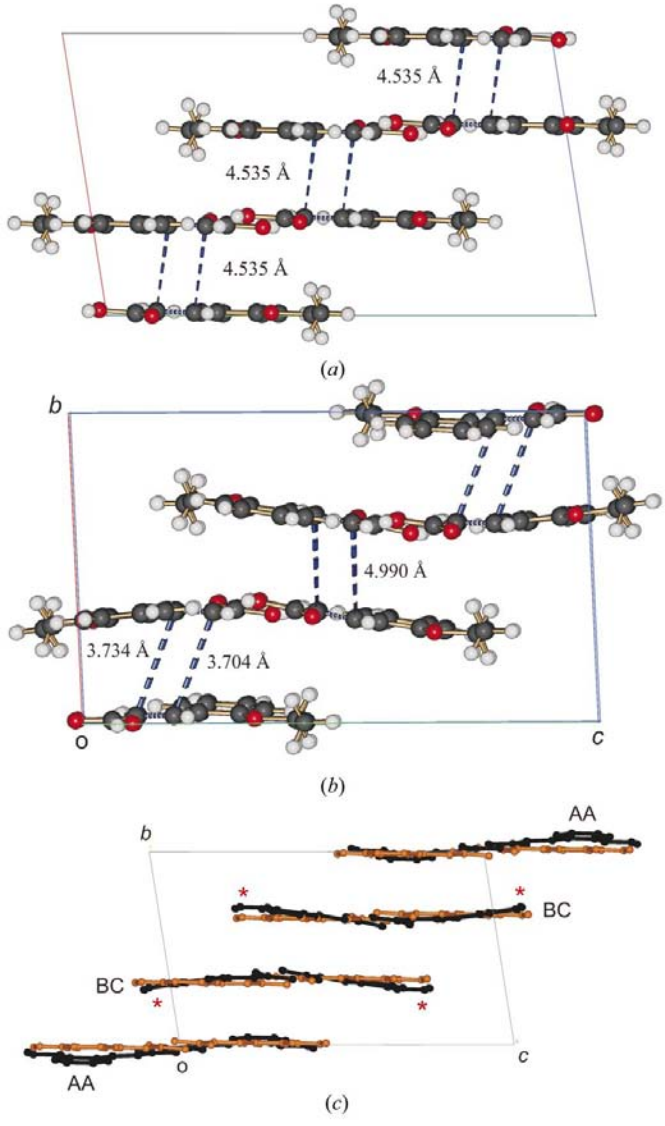

Figure 13
Unit-cell diagrams viewed down the *a*-axis: (*a*) The transformed unit cell of the α-polymorph (α_{trans}) at 173 K; (*b*) the α'-polymorph unit cell at 345 K; (*c*) a superposition of the α_{trans} (in orange) onto the α'-polymorph (in black) from a least-squares fit of corresponding non-H atoms in the *BC* layers of α_{trans} and α'. Ethoxy groups in the *BC* layers point towards the *AA* layers in the α'-polymorph, indicated by an asterix.

transformation indicates that the phase transformation is propagated in a direction perpendicular to the molecular layers. The crystal does not change shape until the transition has propagated about halfway along the crystal. The phase transition therefore involves a combination of molecular conformational changes and centrosymmetric layer shifts.

In contrast, the β-angle remains relatively unchanged, indicating that not much change happens between molecules within an OETCA sheet or layer.

Closely examining the relative orientations of the *AA* and *BC* layers in the α and α'-polymorphs (Fig. 16) gives some insight into the phase transition mechanism. While the ethoxy groups in the *BC* layer overlap with OETCA molecules in the *AA* layers in the α-polymorph (Fig. 16*a*), those in the α'-polymorph lie in voids between the OETCA molecules (Fig. 16*b*). The relative orientations of *AA* and *BC* layers in the two structures indicate that the phase change mechanism involves ethoxy groups in the *BC* layer of OETCA, driving the *AA* layer below it so that the ethoxy groups of molecules in the *BC* layer now lie in voids in the *AA* layer. Ethoxy groups of OETCA molecules in the *AA* layer drive in the opposite direction so that they lie in voids in the *BC* layer (see, for example, the broken arrows in Fig. 16*a*). The phase change can be viewed as one in which the ethoxy groups in the *BC* layer act as levers, pushing the *BC* layer over the *AA* layer and *vice versa* – both motions driving the adjacent *AA* and *BC* layers

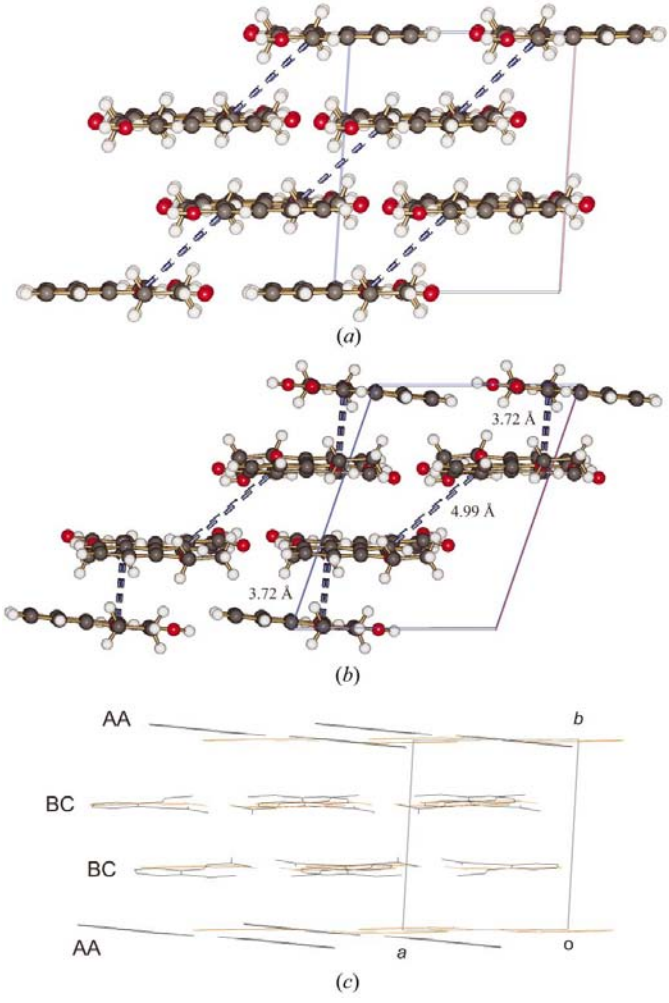

Figure 14
Unit-cell diagrams viewed down the *c*-axis: (*a*) the α-polymorph (α_{trans}) at 173 K; (*b*) the α'-polymorph unit cell at 345 K; (*c*) a superposition of the α_{trans} (in orange) onto the α'-polymorph (in black) (see also the caption to Fig. 13).

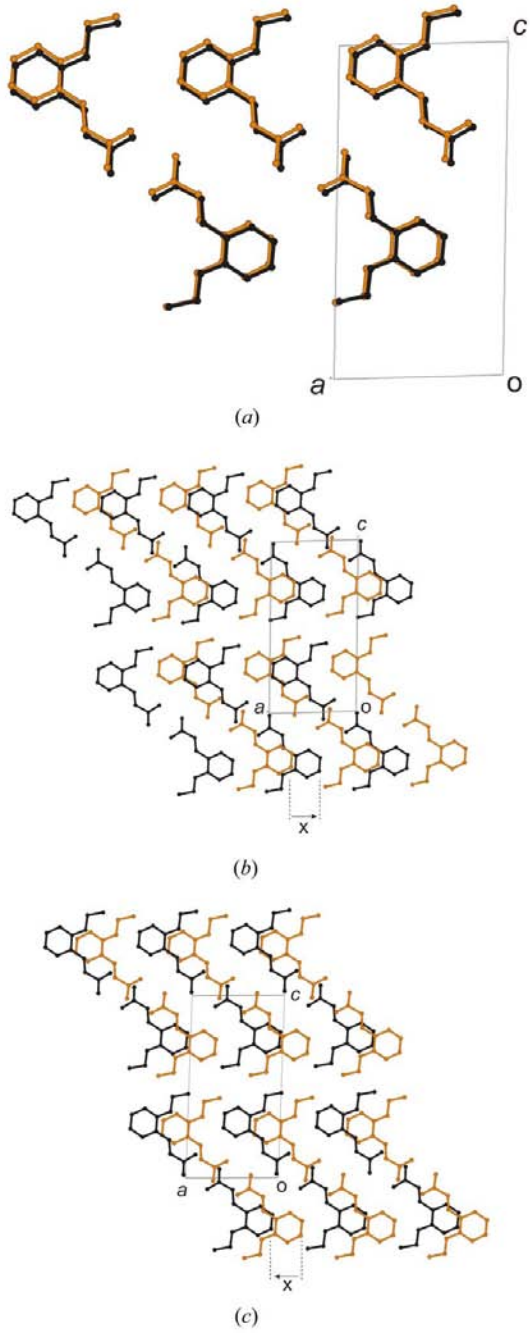

Figure 15
Unit-cell diagrams viewed down the *b*-axis showing a superposition (by least-squares fit as described in Fig. 13) of different layers of the α- and α'-polymorphs: (*a*) the *BC* layers, which are relatively unchanged in the α-(orange) and α'-polymorphs (black) ; (*b*) and (*c*) the lower and upper *AA* layers, respectively, showing a shift of *ca* 2.7 Å of the α'-OETCA molecules relative to the α-*AA* layer (labeled X).

away from each other in a cooperative fashion. In fact, ethoxy groups in the *BC* layers of the resulting α'-polymorph point towards the *AA* layers, as indicated by the asterisks (*) in Fig. 13*c*. The role of voids has been inferred in other studies, such as in the phase transition mechanism for 1-ethyl-3-(4-methylpentanoyl)urea (Hashizume *et al.*, 2003). The relationship between the α- and α'-OETCA polymorphs in the present work seems to be an example of nature modifying a structure to minimize the lattice energy by either accommodating thermal libration as best as possible (at higher temperatures – the minimum energy van der Waals structure becoming less important in this case) or by minimizing van der Waals interactions where thermal libration is less significant (at lower temperatures). The current structure prediction programs tend to use static electrostatic potentials to predict possible structures. Since the dynamic effect of a librating group on a crystal structure is not usually incorporated in the computational model, the existence of structures such as the α'-polymorph would probably not be predicted. Modern crystal structure prediction techniques are however starting to take this into account by evaluating a crystal's mechanical properties (Beyer *et al.*, 2001).

Overlapping the two *BC* layers in the α and α'-polymorphs creates a picture that looks almost identical to Fig. 16(*a*) for both structures. Viewed from above it is obvious why the *BC* layer should move relative to the *A* layer. However, the *BC* layers hardly move relative to each other. A possible explanation is that the ethoxy groups point away from the *BC* layers towards the *AA* layer and therefore do not influence interactions between *BC* layers. The interactions between the two *BC* layers may therefore be dominated by the interplanar van der Waals interactions present in the parent α-polymorph.

Finally, the movement of the *BC* layers with respect to the *AA* layers changes the predimer distance in the *AB* predimer site from 4.54 Å in the α-polymorph to about 3.72 Å in the α'-polymorph. Though small, the relative movement between the *BC* layers changes the predimer distance in the *CC* predimer site from 4.54 Å in the α-polymorph to 4.99 Å in the α'-polymorph (Fig. 9), which will clearly affect solid-state photoreactivity (Fernandes & Levendis, 2004).

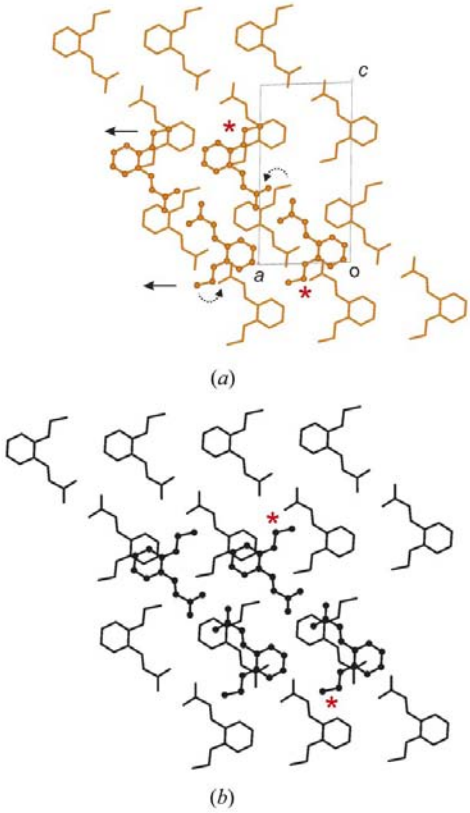

Figure 16
The relative orientation of the *BC* layer (ball and stick representation) to the *AA* layer (stick representation) in (*a*) the α-polymorph and (*b*) the α'-polymorph indicating the difference in the relative positions of the two layers. The position of the OETCA ethoxy group is indicated by an asterix. See text for details.

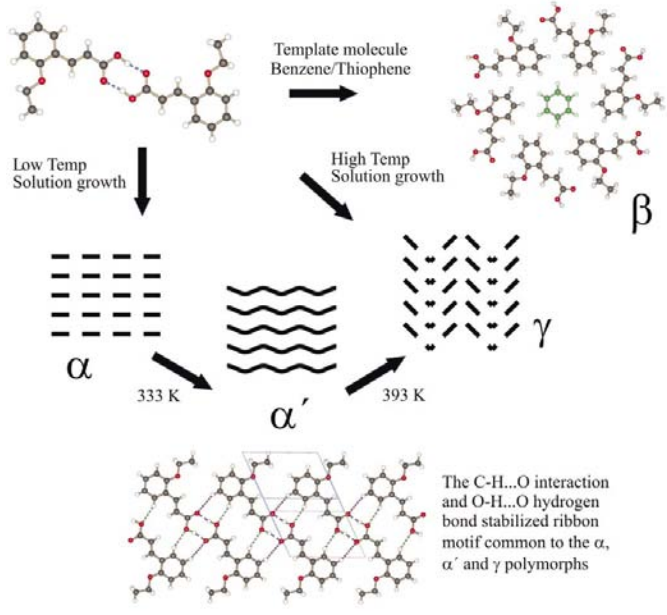

Figure 17
The hydrogen bond and CH···O interaction reinforced ribbon which is the common building block of the α-, α'- and γ-polymorphs.

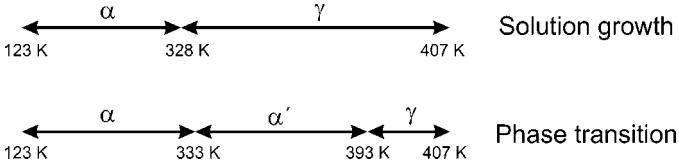

Figure 18
Polymorphs of OETCA obtained from solution (top) or by heating an α-polymorph crystal from 123 K to the melting point at 407 K (bottom). It is not possible to obtain the α'-polymorph from solution. The γ-polymorph can be grown from the melt.

3.9. Relationships between the various OETCA polymorphs

The common building block of all the known polymorphs of OETCA is the OETCA hydrogen-bonded dimer (Fig. 17). Depending on the crystal growing conditions this either assembles around a template molecule (such as benzene) to form the β-solvate structure or one of the ribbon-based OETCA polymorphs (α, α' and γ). OETCA seems to be a unique compound in that the variation of the ribbon-based polymorphs is not so much dependent on the nature of the O—H···O and C—H···O interactions making up the ribbon (the usual emphasis in most polymorph studies), but rather depends on the nature of the van der Waals interactions between the ribbons. The relative stability of the α- and γ-forms is apparent from the solution growth conditions used to obtain each polymorph (Fig. 18). The temperature at which the γ-polymorph becomes accessible from solution crystal growth is *ca* 328 K, while the α-polymorph is obtained at temperatures below this.[3] The γ-polymorph can also be obtained from the melt. This means that the α'-polymorph is only accessible *via* the solid state through the phase transition from the α-polymorph. The α'-polymorph therefore exists only as an energy compromise between the α- and γ-polymorphs – the global high-temperature energy minimum structure represented by the γ-polymorph being kinetically inaccessible *via* the solid state at temperatures below 393 K (Fig. 18).

4. Conclusions

A new polymorph of OETCA (the α'-polymorph) has been discovered and characterized by single-crystal diffraction methods at different temperatures. Noteworthy features of this new crystalline form are summarized below:

(i) α'-OETCA can only be formed by heating α-OETCA above 333 K. It cannot be grown from solution. The α'-form can be stabilized by irradiating α'-OETCA for a short time above 333 K. On cooling, the α'-structure is retained.

(ii) The structure of α'-OETCA ($P\bar{1}$, $Z = 6$) is related to that of the α-OETCA polymorph ($P\bar{1}$, $Z = 2$) as a 'pseudo-supercell' using the matrix $(0\bar{1}0/\bar{1}01/\bar{2}1\bar{1})$. Two of the three independent molecules in the α'-form deviate significantly from planarity resulting in a corrugated-sheet layer structure.

(iii) The α- to α'-phase transformation can be observed optically. On heating, α-OETCA crystals initially 'hop'. Thereafter, there is a reversible single-crystal-to-single-crystal phase transformation, which is accompanied by a significant change in crystal shape and dimensions. The postulated mechanism of the phase transformation requires a cooperative bending motion of the *ortho*-ethoxy groups in every layer into voids of neighbouring layers.

(iv) A remarkable feature of the α'-form is the existence of two different sites that could potentially dimerize on exposure to UV radiation. In one site (the non-centrosymmetric *AB* site) the distance between the double bonds of the predimer is *ca* 3.72 Å, while in the second site (centrosymmetric *CC* site) it is 4.99 Å (in the α-polymorph both sites are the same, with an average distance of 4.54 Å; Fernandes *et al.*, 2001; Gopalan & Kulkarni, 2001). This results in unusual solid-state photodimerization behavior, which will be described in detail in a separate paper (Fernandes & Levendis, 2004).

[3] The exact lower limiting temperature at which the formation of the γ-polymorph becomes favorable is not known. However, work is currently in progress to establish this limiting temperature.

This work was supported by The National Research Foundation of South Africa (GUN 2067413) and the University of the Witwatersrand.

References

Accelrys Inc. (2002). *DS ViewerPro.* Version 5.0. Accelrys Inc., San Diego, California, USA.

Bernstein, J. (2002). *Polymorphism in Molecular Crystals*, p. 223. New York: Oxford University Press.

Bernstein, J., Davis, R. E., Shimoni, L. & Chang, N.-L. (1995). *Angew. Chem. Int. Ed. Engl.* **34**, 1555–1573.

Beyer, T., Day, G. M. & Price, S. L. (2001). *J. Am. Chem. Soc.* **123**, 5086–5094.

Botoshansky, M., Ellern, A., Gasper, N., Henck, J.-O. & Herbstein, F. H. (1998). *Acta Cryst.* B**54**, 277–290.

Bruker (1998). *SMART-NT.* Version 5.050. Bruker AXS Inc., Madison, Wisconsin, USA.

Bruker (1999*a*). *SAINT+.* Version 6.02 (includes *XPREP* and *SADABS*). Bruker AXS Inc., Madison, Wisconsin, USA.

Bruker (1999*b*). *SHELXTL.* Version 5.1 (includes *XS*, *XL*, *XP* and *XSHELL*). Bruker AXS Inc., Madison, Wisconsin, USA.

Busse, G., Tschenter, T., Plech, A., Wulff, M., Frederichs, B. & Techert, S. (2002). *Faraday Discuss.* **122**, 105–117.

Cohen, M. D. & Green, B. S. (1973). *Chem. Brit.* **27**, 490–497.

Cohen, M. D. & Schmidt, G. M. J. (1964). *J. Chem. Soc.* pp. 1996–2000.

Ding, J., Herbst, R., Praefcke, K., Kohne, B. & Saenger, W. (1991). *Acta Cryst.* B**47**, 739–742.

Enjalbert, R. & Galy, J. (2002). *Acta Cryst.* B**58**, 1005–1010.

Enkelmann, V., Wegner, G., Novak, K. & Wagener, K. B. (1993). *J. Am. Chem. Soc.* **115**, 10390–10391.

Etter, M. C. (1990). *Acc. Chem. Res.* **23**, 120–126.

Fernandes, M. A. & Levendis, D. C. (2004). *Acta Cryst.* B**60**, 315–324.

Fernandes, M. A., Levendis, D. C. & de Koning, C. B. (2001). *Cryst. Engng*, **4**, 215–231.

Gopalan, R. S. & Kulkarni, G. U. (2001). *Proc. Indian Acad. Sci. (Chem. Sci.)* **113**, 307–324.

Hashizume, D., Miki, N., Yamazaki, T., Aoyagi, Y., Arisato, T., Uchiyama, H., Endo, T., Yasui, M. & Iwasaki, F. (2003). *Acta Cryst.* B**59**, 404–415.

Hosomi, H., Ito, Y. & Ohba, S. (2000). *Acta Cryst.* B**56**, 682–689.

Hostettler, M., Birkedal, H., Gardon, M., Chapuis, G., Schwarzenbach, D. & Bonin, M. (1999). *Acta Cryst.* B**55**, 448–458.

Hung, J. D., Lahav, M., Luwisch, M. & Schmidt, G. M. J. (1972). *Isr. J. Chem.* **10**, 585–599.

Ito, Y., Kitada, T. & Horiguchi, M. (2003). *Tetrahedron*, **59**, 7323–7329.

Kaftory, M., Botoshansky, M., Kapon, M. & Shteiman, V. (2001). *Acta Cryst.* B**57**, 791–799.

Katrusiak, A. (2000). *Acta Cryst.* B**56**, 872–881.

Keller, E. (1997). *SCHAKAL*-97. University of Freiberg, Germany.

Lieberman, H. F., Davey, R. J. & Newsham, D. M. T. (2000). *Chem. Mater.* **12**, 490–494.

Ohba, S. & Ito, Y. (2003). *Acta Cryst.* B**59**, 149–155.

Spek, A. L. (2003). *J. Appl. Cryst.* **36**, 7–13.

Tanaka, K. & Toda, F. (2000). *Chem. Rev.* **100**, 1025–1074.
Varshney, D. B., Papaefstathiou, G. S. & MacGillivray, L. R. (2002). *Chem. Commun.* pp. 1964–1965.
Wilson, C. C. (2001). *Chem. Phys. Lett.* **335**, 57–63.
Wilson, C. C., Shankland, N. & Florence, A. J. (1996*a*). *Chem. Phys. Lett.* **253**, 103–107.
Wilson, C. C., Shankland, N. & Florence, A. J. (1996*b*). *J. Chem. Soc. Faraday Trans.* **92**, 5051–5057.